Method for Studying Orientation Variations Near Surfaces in Semicrystalline Polymers

C. P. BUCKLEY, *Polymer Engineering Division, Department of Mechanical Engineering, UMIST, Manchester, M60 1QD, United Kingdom*, and
R. J. TAYLOR, *Physics Department, Christie Hospital and Holt Radium Institute, Withington, Manchester, M20 9BX, United Kingdom*

Synopsis

The method of grazing incidence X-ray diffraction provides a convenient means of examining crystal orientation close to the surface of a semicrystalline polymer. Since the sampled depth is governed by the choice of X-radiation (via its absorption coefficient) and the angle of incidence, it is under the control of the experimenter. The method was tested and shown to be valid by applying it to a crossply laminated film of oriented polyethylene, of thickness 50 μm, in which the different crystal orientations on opposite faces of the film were known. Further experiments, with two polyethylene films of 20 μm and 40 μm thickness each extruded with differing rates of cooling on each surface, demonstrated the ability of the method to resolve spatial variations of orientation on this scale arising during manufacture.

INTRODUCTION

During a recent study of extruded polyethylene films, we succeeded in resolving substantial variations in the degree of molecular orientation through films of 40 μm thickness and even less. Such resolution was achieved without the need for sectioning, by using conventional wide-angle X-ray diffraction (WAXD), but with the X-ray beam at *grazing* incidence. Although this method does not seem to have been applied to polymers before, we believe it is a potentially powerful tool for studying any semicrystalline polymer product where orientation variations close to a flat surface need to be determined. It is well known that such variations are common in melt-processed polymers, and reflect gradients of temperature and strain-rate history in the melt during processing.

Our purpose here is to discuss the principles of grazing incidence WAXD and its quantitative interpretation, to give some practical details of how it may be applied to measuring near-surface orientation in polymers, and to present some illustrative results for the polyethylene films. A fuller report on the microstructure of the films will be given elsewhere.

First, to put the method into perspective, it may be helpful to review briefly the few other techniques available for detecting through-thickness variations of orientation, and their limitations.

Birefringence at the surface of a polymer film can be deduced from the principal refractive indices at the surface. These are conveniently measured via the critical angles of incidence for a glass/polymer interface, using an Abbé refractometer with polarised light, as shown by Schael[1] and Tanaka, Masuko, and Okajima[2,3] for polyolefine films. In correct operation,* the refractometer

* Tanaka et al.[2,3] have shown that light scattering within a polymer film can give rise to artifacts with this technique. Two cutoffs may be seen, one arising from each film surface.

Journal of Applied Polymer Science, Vol. 29, 1985–1998 (1984)
 CCC 0021-8995/84/061985-14$04.00

measures the minimum refractive indices of an inhomogeneous film. For quenched polymer films these will usually occur at one of the surfaces. The birefringence so obtained can then be compared with the mean through the thickness of the film, as measured in the usual manner in transmitted light with a compensator, to give an indication of any difference in birefringence between the surface and interior.

Another method which provides a surface measurement for comparison with a bulk measurement is attenuated total reflection infrared dichroism, as suggested by Flournoy[4] and developed further by Sung.[5] This is a true surface measurement, since the radiation interacts with the polymer only through total external reflection at a polymer/crystal interface, and therefore penetrates the polymer only to a depth of the order of its wavelength (e.g., see Harrick[6]).

A further approach is to examine sections by X-ray diffraction, localizing the region sampled by the X-rays by either (a) using a fine beam or (b) using sections cut thinly in the direction normal to the surface of interest. Such methods have been used by several authors[7–9] to reveal variations in crystal orientation through the thickness of injection mouldings. In practice, however, resolution is limited to about 100 μm by the spread of the beam in (a) or the thickness of the section in (b), whereas in many polymer products (fibres and films) the entire thickness is less than this.

Better spatial resolution within sections can be obtained by using optical methods, since advantage can then be taken of optical microscopy. Thus birefringence measurements on such sections are possible, if they are transparent, but can be hampered by the difficulty of cutting sections of sufficiently uniform thickness and by errors in measuring the thickness. Moreover, all methods involving the cutting of sections are prone to artifacts caused by damage to the polymer during sectioning.

When specimens are in the form of fibers, radial variations in birefringence are sometimes clearly visible in the optical microscope.[10] In such cases, however, it is not possible to make unambiguous quantitative measurements, because refraction effects caused by the cylindrical fiber geometry distort the image.[11]

Clearly, none of these techniques allows orientation variations to be measured close enough to the surface to be of help in the quantitative study of fibers or films, or of moldings in which the surface structure is of greatest importance. Our solution, as mentioned above, has been to use WAXD at grazing incidence. This allows quantitative measurements, sampling at different depths from the surface, without any need to section the specimen. The latter advantage is crucial in the study of soft thermoplastics such as polyethylene. It is made possible (for any specimen thickness) by collecting the diffracted beam emerging on the same side of the specimen as the incident beam, i.e., by obtaining the WAXD pattern in reflection mode, the procedure more commonly associated with metals.

GRAZING INCIDENCE X-RAY DIFFRACTION

As is well known, a beam of X-rays which traverses a path of length l through a material is attenuated from its incident intensity I_0 to an intensity I given by

$$I = I_0 \exp(-\mu l) \tag{1}$$

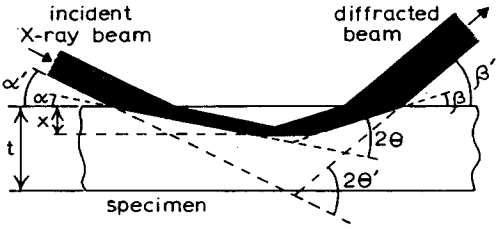

Fig. 1. Principle of the grazing incidence X-ray diffraction experiment: the glancing angle α^1 is made small.

where μ is the linear absorption coefficient for the particular material concerned, at the appropriate X-ray wavelength. Values of μ for metals are generally much higher than for polymers, since the latter tend to consist of lighter elements. For example, with the commonly used Cu Kα X-rays, $\mu \simeq 260$ mm^{-1} for iron whereas $\mu \simeq 0.35$ mm^{-1} for polyethylene. This means that any reflection X-ray diffraction experiment on a metal specimen penetrates at most only the outer few micrometers at the surface of the specimen, whereas with a polymer specimen the X-ray penetration is much deeper for the same angle of incidence. There are, however, two ways in which the depth of penetration can be decreased, in order to adapt the reflection method for examining surface layers of polymer specimens. First, the angle of incidence can be made almost 90°, so that the glancing angle between incident beam and specimen surface is very small, i.e., with the specimen virtually edge-on to the incident beam. This reduces the penetration depth by increasing the X-ray path length l in the specimen for diffraction from a given depth. Second, X-rays of higher wavelength can be used, resulting in a higher value for μ and hence more rapid attenuation. Clearly, the most effective approach would be to combine these two methods. Progress in this direction has been described by Herglotz, who obtained small-angle X-ray scattering patterns from the surface layers of poly(ethylene terephthalate) films using edge-on specimens and the "soft" X-radiations Al Kα (wavelength λ = 0.834 nm)[12] and C Kα (λ = 4.47 nm).[13]

Precisely the same principles can be applied to WAXD, for the study of crystal lattice orientation near polymer surfaces. The following is an outline of the factors involved in quantitative interpretation of WAXD patterns so obtained.

Consider the situation shown in Figure 1. An X-ray beam of intensity I_0 is incident upon the flat surface of a specimen of thickness t at a glancing angle α^1, which is reduced by refraction to a slightly smaller angle α within the specimen. Unit cross-sectional area of the incident beam therefore illuminates a patch of area $1/\sin \alpha^1$ on any plane parallel to the surface. It is diffracted along a direction inclined at an angle β to the surface, which enlarges to β^1 on exit from the specimen, and therefore contributes an area $\sin \beta^1/\sin \alpha^1$ to the emergent diffracted beam.

The deviations of the beam by refraction, although small, cannot be neglected when α or β is less than ca. 1°. In the case of the incident beam, for example, the relationship between α^1 and α, for small α, is as follows:

$$\alpha^1 \simeq (\alpha^2 + \alpha_c^2)^{1/2} \tag{2}$$

where α_c is the critical angle for total reflection. From the theory for dispersion

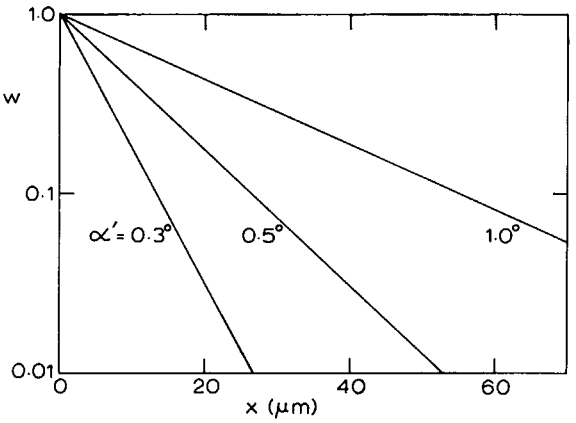

Fig. 2. Weighting function W vs. depth x within the specimen, as given by eq. (5) for diffraction of Fe Kα X-rays from (200) planes in polyethylene, at various glancing angles of incidence α^1 (see Fig. 1).

of X-rays (see, for example, Compton and Allison[14]), it can be shown that when X-rays of wavelength λ are incident on polyethylene of density ρ, α_c is given in degrees by

$$\alpha_c = 3.16 \times 10^7 \lambda \rho^{1/2} \tag{3}$$

In the example of Fe Kα X-rays, used in the present work, incident on a specimen of polyethylene with $\rho = 945$ kg/m^3 (typical of films used in this work) eq. (3) yields $\alpha_c = 0.19°$.

When the incident X-rays interact with unit volume of the specimen at a depth x, let the intensity fraction diffracted in a particular direction, by crystals in the appropriate orientation, be $f(x)$. The emerging diffracted intensity contributed by unit depth, dI/dx, can then be expressed as follows, by application of eq. (1):

$$\frac{dI}{dx} = \frac{I_0}{\sin \beta^1} W(x) f(x) \tag{4}$$

where

$$W(x) = \exp\left[-\mu x \left(\frac{1}{\sin \alpha} + \frac{1}{\sin \beta}\right)\right] \tag{5}$$

The weighting function $W(x)$ clearly weights diffraction from crystals near the surface ($x = 0$) most strongly, but the degree of discrimination is under the

TABLE I
Data for Four Candidate X-Ray Sources for Grazing Incidence X-Ray Diffraction from (200) Planes in Polyethylene of Density $\rho = 945$ kg/m^3 [a]

Radiation	Mo Kα	Cu Kα	Fe Kα	Cr Kα
λ (nm)	0.0711	0.1542	0.1937	0.2291
μ (mm^{-1})	0.0484	0.347	0.698	1.177
$2\theta^\circ_{200}$	11.0	24.1	30.3	36.1

[a] Relevant X-ray wavelengths λ and mass attenuation coefficients μ/ρ were taken from Ref. 16, and the a lattice parameter for polyethylene was assumed to be 0.740 nm.[17]

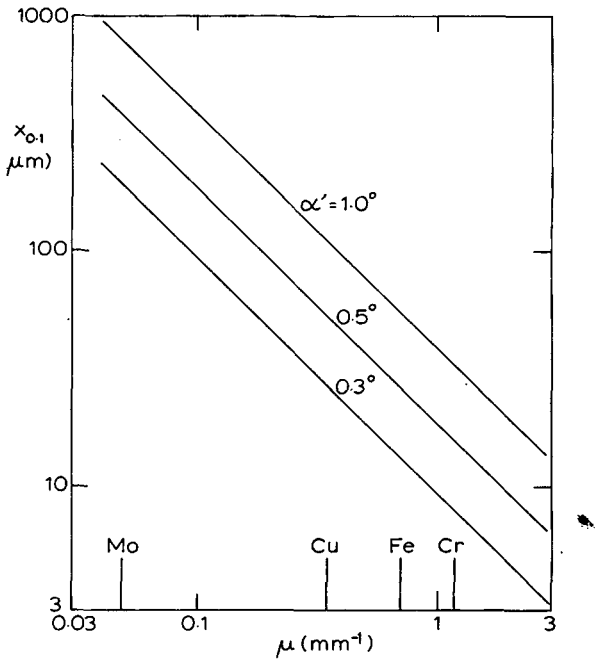

Fig. 3. Log–log plot of penetration depth $x_{0.1}$ vs. linear absorption coefficient μ, for grazing incidence X-ray diffraction from (200) planes in polyethylene (see Fig. 1). Also shown are the values of μ applying to the four commonly used Kα radiations referred to in Table I.

control of the experimenter by varying α^1 or β^1, or even by varying μ by changing the X-ray wavelength. An illustration of the discrimination provided by $W(x)$, and its variation with α^1, is given in Figure 2. The example shown is for diffraction of Fe Kα X-rays (λ = 0.194 nm) from (200) planes of polyethylene (2θ = 30.3°). The specimen is assumed to be a film oriented as in Figure 1, i.e., with a coplanar arrangement of incident beam, diffracted beam, and surface normal, such that $\beta = 2\theta - \alpha$. Figure 2 shows immediately that, provided small glancing angles are used ("grazing incidence"), the diffraction pattern will arise predominantly from crystals near the surface of the specimen. Furthermore, the depth of penetration can be conveniently controlled by simply varying α^1. A measure of the penetration depth is the depth x_p at which W has decreased to some fraction p, say 0.1, of its value (unity) at the surface $x = 0$. This is given by rearranging eq. (5) as follows:

$$x_p = 2.303 \log\left(\frac{1}{p}\right) \Big/ \mu \left(\frac{1}{\sin\alpha} + \frac{1}{\sin\beta}\right) \tag{6}$$

Equation (6) shows clearly that the penetration depth is reduced by increasing μ. An important experimental variable, therefore, is the choice of suitable X-radiation. Since absorption coefficients increase with increasing wavelength, this implies the use of X-rays of long wavelength if shallow penetration is required. In the case of WAXD, however, the wavelength is clearly limited to values less than twice the lattice spacing of interest; otherwise, Bragg's law dictates that diffraction will be unobtainable. For (200) planes of polyethylene, for example, this places an upper limit on λ of 0.74 nm. In addition, there is the

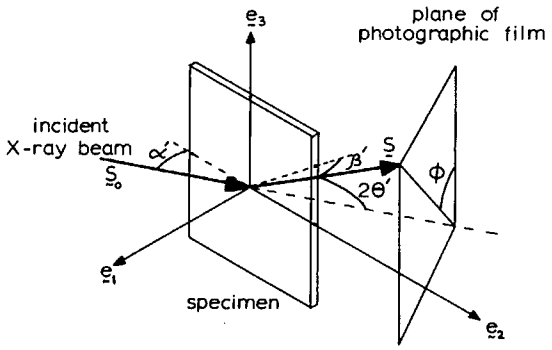

Fig. 4. Schematic diagram of the grazing incidence X-ray diffraction experiment, for a general azimuthal angle ϕ on the diffraction pattern. Unit vectors $\mathbf{S}_0$ and $\mathbf{S}$ define the direction of incident and diffracted beams respectively, while $\mathbf{e}_1$, $\mathbf{e}_2$, and $\mathbf{e}_3$ are mutually perpendicular unit vectors defining directions with respect to the specimen surface.

practical constraint that only certain X-radiations are readily available from commercial X-ray tubes: to use others, it is necessary to resort to purpose-built X-ray generators, for example, a generator with interchangeable targets as described by Herglotz.[12] Again with (200) diffraction from polyethylene as the example, relevant details for four common target elements are given in Table I. The effect that changing μ has on the depth of penetration is illustrated in Figure 3. Of the four radiations whose μ values are included in Figure 3, molybdenum and copper give insufficient resolution for the present application. Chromium gives the greatest resolution, but iron is also acceptable.

The discussion so far has assumed the configuration shown in Figure 1, where the incident beam, diffracted beam, and surface normal are coplanar. In the study of crystal orientation, however, interest centers on how the intensity varies around the cone of diffracted X-rays. Consider, therefore, the more general arrangement sketched in Figure 4. The specimen surface is vertical but rotated away from the horizontal incident beam by the glancing angle α^1. Diffracted X-rays are collected by a flat photographic film placed behind the specimen, normal to the incident beam. The azimuthal angle, ϕ is 90° for points on the equator of the diffraction patterns—the situation depicted in Figure 1.

The Appendix shows that for a general point on the diffraction cone (a general value of ϕ) β^1 is given by the expression

$$\sin \beta^1 = \sin 2\theta^1 \cos \alpha^1 \sin \phi - \cos 2\theta^1 \sin \alpha^1 \tag{7}$$

where $2\theta^1$ is the scattering angle modified by the relatively much smaller deflection due to refraction (see Figure 1—in this case $2\theta^1 = 2\theta + \alpha^1 - \alpha + \beta^1 - \beta$). In practice it is usually sufficiently accurate to neglect the latter in comparison to 2θ and to assume $2\theta^1 \simeq 2\theta$. As ϕ decreases from 90° towards zero, therefore, β^1 decreases from its initial value of $2\theta^1 - \alpha^1$ until finally it reaches the critical angle α_c at

$$\phi = \arcsin(\alpha^1 \cot 2\theta^1 + \alpha_c \csc 2\theta^1) \tag{8}$$

where we have assumed both α^1 and α_c are small angles (and are expressed in

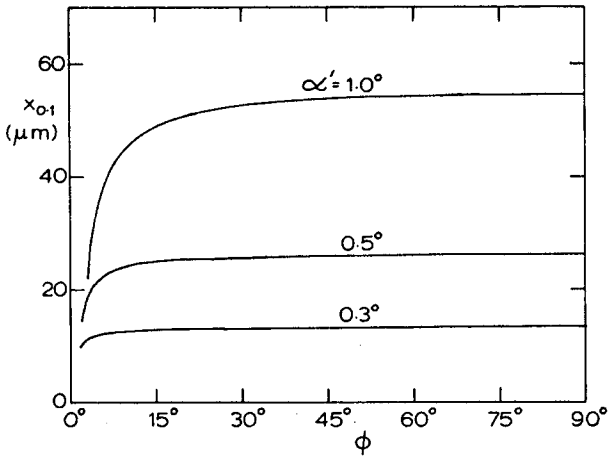

Fig. 5. Penetration depth $x_{0.1}$ vs. azimuthal angle ϕ, as given by eqs. (6) and (7) for grazing incidence X-ray diffraction of Fe Kα X-rays from (200) planes in polyethylene (see Fig. 4).

radians). With further decrease in ϕ the diffracted beam cannot escape from the specimen, and the registered diffraction ring will show a cutoff at the value of ϕ given by eq. (8) [e.g., at $\phi = 2.1°$ for $\alpha^1 = 1°$ incidence Fe Kα X-rays diffracted by (200) planes of polyethylene]. In practice experimental factors, such as unevenness of the specimen surface and the limit of detection on the photographic film, may combine to cause this cutoff to appear at a larger value of ϕ.

A more serious consequence of the variation of β^1 with ϕ is that the weighting given to different depths $W(x)$ will also vary with ϕ [see eq. (5)]. This might be expected to cast doubt on the validity of the method for studying orientation, since it is precisely the variation of intensity around diffraction rings which reveals preferred orientation of crystal planes. In practice the problem is not likely to be serious: the depth of X-ray penetration is not significantly reduced as ϕ decreases, until it is as low as about 10°, as illustrated in Figure 5.

Finally, to apply the method described here to the study of orientation, it is necessary to know the direction of plane normals giving rise to diffraction at any particular point on a diffraction ring. As shown in the Appendix, unit normal $\mathbf{n}$ to any plane diffracting to a point on a ring with azimuthal angle ϕ is given as follows (neglecting here the small deflections due to refraction):

$$\mathbf{n} = (\cos\theta \sin\phi \cos\alpha + \sin\theta \sin\alpha)\mathbf{e}_1 + (\cos\theta \sin\phi \sin\alpha - \sin\theta \cos\alpha)\mathbf{e}_2 + \cos\theta \cos\phi\, \mathbf{e}_3 \quad (9)$$

in terms of the orthogonal unit vectors $\mathbf{e}_1$, $\mathbf{e}_2$, $\mathbf{e}_3$ defined in Figure 4.

If the specimen is rotated about $\mathbf{e}_1$ to obtain a series of diffraction patterns, the only directions of $\mathbf{n}$ within the specimen from which it is impossible to register diffraction are those inclined to the surface normal by less than $\theta - \alpha$ or more than $\arccos[\sin\alpha(\cos\theta \cot 2\theta + \sin\theta)]$. For the case of 1° incidence in the example used earlier in this section, these angles are 14° and 88°, respectively. This is not likely to be an excessive gap in the information available, for many studies of orientation.

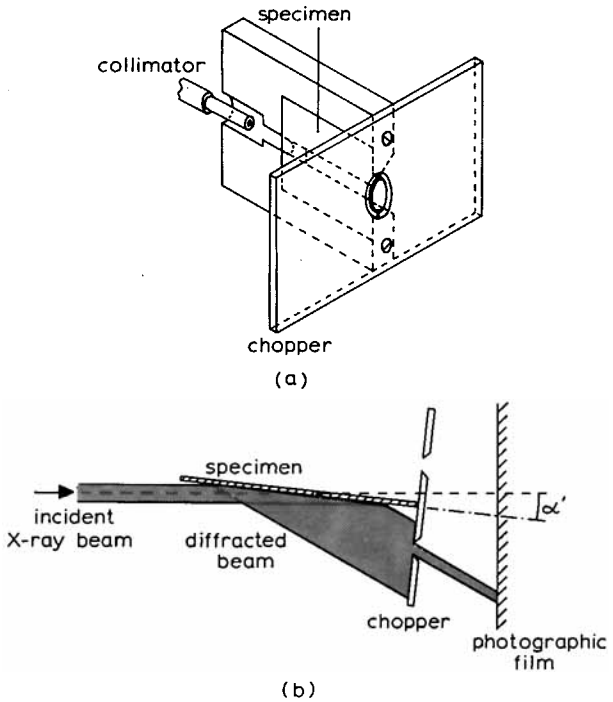

Fig. 6. Experimental arrangement for grazing incidence X-ray diffraction from polyethylene films: (a) sketch of specimen holder; (b) cross section in plan view, showing function of the beam "chopper."

EXPERIMENTAL DETAILS

To carry out grazing incidence WAXD on polymer films, we employed the T-shaped specimen holder sketched in Figure 6(a). The film specimen was held flat by a layer of adhesive tape against a thin glass cover slip, itself bonded to a flat brass plate. To accommodate the small glancing angles of incidence involved in these experiments, the brass plate was recessed to allow for close approach of the X-ray collimator as shown. At the other end of the specimen holder, the transverse plate with an annular hole at its center was employed to "chop" the diffracted beam. Since the collimator provided an incident beam of width 1 mm, at low glancing angles it illuminated a large area of the specimen, producing a very wide diffracted beam. The annular "chopper" served to cut down the diffracted beam reaching the photographic film, thereby selecting X-rays from only one small area of the specimen, in the manner sketched in Figure 6(b). For the experiments reported here, the annular gap was of inner radius 3.0 mm, width 0.5 mm, and the distance from chopper to photographic film was 30 mm. The entire specimen holder was clamped on a goniometer, which was in turn mounted on the rotatable stage of the X-ray camera. A vernier scale allowed rotation of the stage to be read to 0.1°. The camera was used with a source of Fe Kα X-rays, for reasons given in the previous section.

Exposure times were typically of the order of 24 h. These were necessitated by the high absorption and consequent low intensity of the emerging X-ray beam.

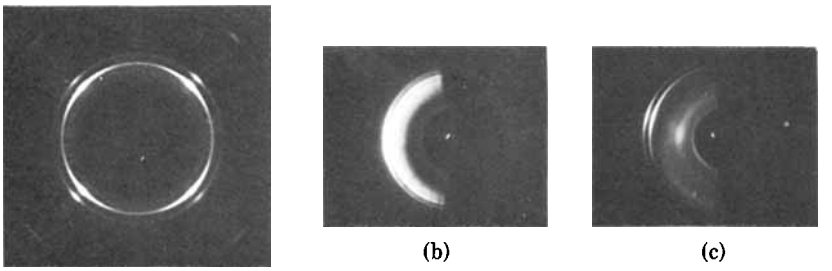

(a) (b) (c)

Fig. 7. X-ray diffraction patterns from film L. Patterns obtained as follows: (a) transmission at normal incidence; (b) reflection at $\alpha^1 = 3.0°$; (c) reflection at $\alpha^1 = 0.3°$. (Machine direction MD is vertical in each case.)

It is clear from Figure 2 that the total diffracted intensity from the specimen [see eq. (4)]

$$I = \frac{I_0}{\sin \beta^1} \int_0^t W(x) f(x)\, dx \tag{10}$$

will decrease rapidly as α^1 decreases, reaching zero when $\alpha^1 = \alpha_c$.

In this paper we report results obtained with just three polyethylene films. They were all produced as tubes by melt extrusion from Unifos DMDS 2912 high density polyethylene (HDPE). Their characteristic features were as follows.

Film L. This film was a crossply laminate, consisting of two identical films, each 20 μm thick, highly oriented by drawdown from the die during extrusion. They were bonded together by a 10 μm layer of HDPE laminant with their orientation axes inclined at +45° and −45° to the machine direction (MD) of the laminate.

Film A. This film was a single layer 20 μm thick, air-cooled on both surfaces during extrusion, and again oriented by drawdown, with molecular orientation parallel to the MD.

Film B. This film was of thickness 40 μm, but otherwise similar to film A, except that during extrusion it had received enhanced cooling on its inner surface. Again the molecular orientation axis was parallel to the MD.

The unusual crossply laminated film L was included in this study because it provided an unambiguous test of the effectiveness of the method described here. Since the two molecular orientation axes lay at right angles, diffraction from each surface could be readily identified in the diffraction patterns. Films A and B formed part of a wider study of the effects of extrusion conditions on the microstructure of HDPE films. Further details will be given elsewhere.

RESULTS

Crossply-Laminated Film. The orientation in film L can be readily appreciated from Figure 7(a). This shows the WAXD pattern as usually obtained, in transmission mode, with the incident beam normal to the film and the MD vertical. For this crossply laminate, it is clear that the prominent ($hk0$) diffraction is preferentially confined to two planes, inclined at ±45° to the MD (the 10 μm layer of presumably unoriented HDPE laminant appearing not to con-

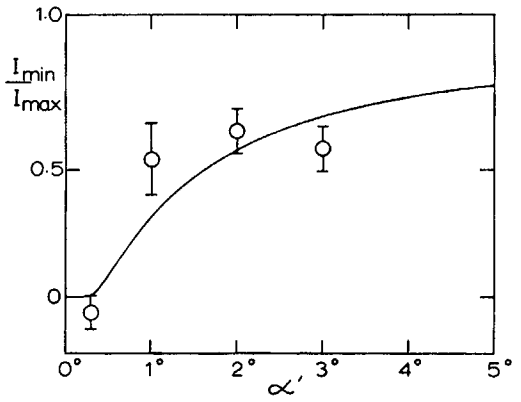

Fig. 8. Intensity ratio I_{min}/I_{max} of (200) diffraction peaks obtained in grazing incidence X-ray diffraction from film L, at various glancing angles α^1. Also shown is the curve predicted by eq. (12).

tribute significantly). (200) diffraction is the outer of each of the prominent pairs of arcs.

Now suppose that the film is mounted as shown in Figure 4, with the MD vertical (i.e., parallel to $\mathbf{e}_3$) and examined in reflection mode, with the incident beam almost edge-on. The diffraction pattern obtained at $\alpha^1 = 3.0°$ is shown in Figure 7(b). The reader will note that the two sets of ($hk0$) diffraction arcs are now centered at more than 45° to the meridian. In fact, it can be shown (see Appendix) that ($hk0$) diffraction at Bragg angle θ will now appear on the photographic film in two directions inclined at

$$\phi^* = \pm \arccos(\tan \theta) \tag{11}$$

to the meridian of the diffraction pattern. For (200) diffraction of Fe Kα X-rays from polyethylene $\phi^* = \pm 74.3°$.

In Figure 7(b) and subsequent diffraction patterns obtained at grazing incidence there are some unusual features worthy of comment. The reader will note that only the left-hand half of the pattern is visible (faint features on the right-hand half are artifacts from the specimen holder). This is the half corresponding to the reflected beam, the transmitted beam having been lost by absorption in the glass cover slip behind the film specimen. The glass contributes the strong "amorphous halo" prominent in Figure 7(b). A cutting off of the pattern a few degrees to the left of the meridian, as predicted above, is clearly visible. These may instead, however, be the shadows of the thin brass connections between the inner and outer halves of the annular chopper, which were located on the meridian.

The special manner in which the laminate was constructed meant that the two sets of ($hk0$) diffraction maxima visible in Figure 7(b) originated from opposite faces of the film. A quantitative measure of the X-ray penetration of the furthest face of the laminate, compared with that of the nearest face, was provided by the ratio of the intensities of the least intense (200) maximum (from the furthest face) to the most intense (from the nearest face): I_{min}/I_{max}. (200) peak intensities were measured by microdensitometer and corrected for peak overlap, and the ratio I_{min}/I_{max} determined for a few values of glancing angle α^1. Results are

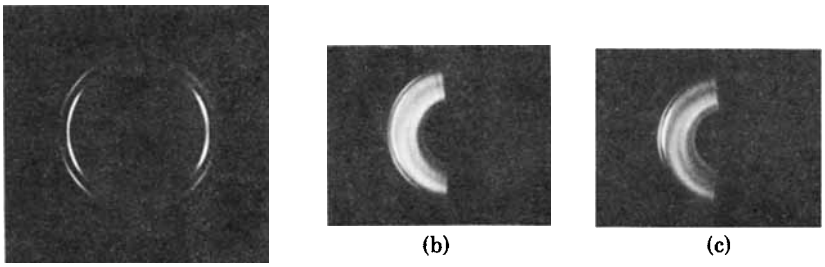

(a) (b) (c)

Fig. 9. X-ray diffraction patterns from film A. Patterns obtained as follows: (a) transmission at normal incidence, on a cross section cut perpendicular to the transverse direction of the film; (b) reflection at $\alpha^1 = 0.3°$ from the inner surface of the film; (c) reflection at $\alpha^1 = 0.3°$ from the outer surface of the film. (MD is vertical and film normal is horizontal in each case.)

plotted in Figure 8. Also shown (solid line) is I_{min}/I_{max} as predicted by the theory given above, as follows. If both surface layers of the laminate are assumed homogeneous and highly oriented, and diffraction from the laminant is neglected, then f can be assumed zero at all points on the diffraction ring except at the positions $\phi = \pm 74°$. At these two points $f(x)$ will be given as follows:

$$\text{at } \phi = +74°, \quad \begin{cases} f = f_0, & 0 < x < 20\ \mu\text{m}, \\ f = 0, & 20 < x < 50\ \mu\text{m}, \end{cases}$$

$$\text{at } \phi = -74°, \quad \begin{cases} f = 0, & 0 < x < 30\ \mu\text{m}, \\ f = f_0, & 30 < x < 50\ \mu\text{m} \end{cases}$$

where f_0 is a constant. Substituting into eq. (10) and carrying out the integration, we obtain

$$\frac{I_{min}(\phi = -74°)}{I_{max}(\phi = +74°)} = \frac{W(30\ \mu\text{m}) - W(50\ \mu\text{m})}{1 - W(20\ \mu\text{m})} \tag{12}$$

Fiqure 8 shows clearly the predicted extinguishing of diffraction from the furthest face of the laminate as α^1 approaches zero. Figure 7(c) shows the WAXD pattern for $\alpha^1 = 0.3°$, where diffraction from the furthest face has disappeared completely. As can be seen, however, there is not complete agreement between I_{min}/I_{max} as measured and as predicted by theory. There are at least two reasons for this. First, there was probably unevenness of the surface of the film (and hence variations in α^1) on a scale sufficient to explain the discrepancy. Second, since the two component films of the laminate were themselves likely to be inhomogeneous (see below), the assumption of f being independent of x within each film is open to question. Notwithstanding this quantitative discrepancy, these results for the laminated film demonstrate unequivocally the variation in depth of X-ray penetration with varying α^1, which is the notable advantage of this method.

Film A. For comparison with the surface information provided by grazing incidence WAXD, "conventional" transmission diffraction patterns were obtained at normal incidence, from sections cut normal to the transverse direction of the film. They indicate the mean level of orientation in the film, as viewed with the X-ray beam edge-on, since all depths from the surface to center are

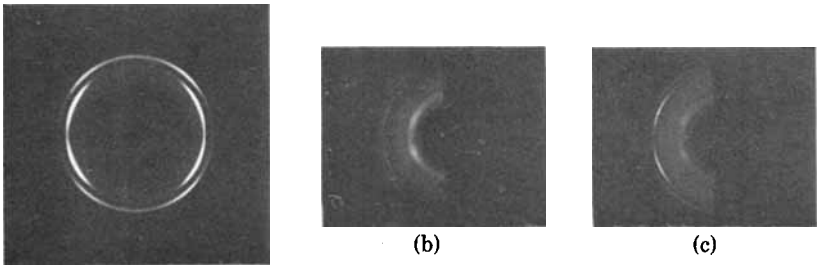

Fig. 10. As Figure 9, but for film B.

weighted equally. A WAXD pattern obtained in this way with film A is shown in Figure 9(a). The extent of orientation which it reveals is characteristic of HDPE crystallized under an intermediate degree of melt draw.[15] Crystal b-axes are aligned preferentially perpendicular to the MD, while a and c maxima are inclined at less than 90° to the MD. Now compare Figure 9(a) with the patterns obtained in reflection by grazing incidence WAXD. These are given in Figures 9(b) and 9(c), for the inner and outer surfaces of the air-cooled tubular film, respectively. In both cases the glancing angle $\alpha^1 = 0.3°$, and hence the observed diffraction originated close to the film surfaces (see Fig. 2). What is most striking is that the patterns given in Figures 9(a), 9(b), and 9(c) are all different. The degree of orientation of c-axes parallel to the MD increases in the sense 9(a) → 9(b) → 9(c). It is clear that the surface layers [Figs. 9(b) and 9(c)] have a higher degree of c-axis orientation than the interior [included in Fig. 9(a)]. Moreover, the outer surface of the film [Fig. 9(c)] shows higher c-axis orientation than the inner surface [Fig. 9(b)]. The likely explanation for these differences is that the most rapidly cooled parts of the film crystallize first, and hence carry the highest stress during crystallization. They are therefore left with the highest degree of crystal orientation. It is to be expected that the surface regions of the film, especially the outer surface, would cool faster than the interior of the film during extrusion.

Film B. A "conventional" transmission WAXD pattern, obtained in the same manner as Figure 9(a), is shown in Figure 10(a) for the film with enhanced cooling—film B. Again it is indicative of an HDPE film crystallized under a moderate degree of melt orientation.

For comparison, the WAXD patterns obtained in reflection at grazing incidence are shown in Figures 10(b) and 10(c), for the inner and outer surfaces of the film, respectively. In both cases $\alpha^1 = 0.3°$. The most striking differences in orientation are between Figures 10(b) and 10(c), with 10(b) showing a higher degree of c-axis orientation than 10(c). It is interesting to note that this is in the opposite sense compared to film A, extruded without the additional cooling. These patterns show that enhancing the cooling of the inner surface of the film has increased the degree of orientation at this surface, relative to the outer surface. The explanation is the same as before. In this case it is the inner surface of the film which was the first to crystallize and hence carried the highest stress during crystallization.

CONCLUSIONS

In conclusion, the method of WAXD at grazing incidence is an effective means of studying spatial variations of the degree of molecular orientation, within the first few tens of micrometers from the surface of a semicrystalline polymer. This method has several advantages. It is nondestructive and can be carried out using standard WAXD cameras, with the simple addition of a special specimen holder. Quantities such as $x_{0.1}$ can be used to provide quantitative measures of the depth of X-ray penetration at this level of resolution, provided glancing angles of incidence of the order of 1° or less are achievable. The depth of penetration can be varied simply by varying the glancing angle. This has been clearly demonstrated here, by the results obtained with a crossply-laminated film of HDPE.

We believe that the method is especially useful for examining the effects of manufacturing conditions on the state of orientation near the surface of solid polymer products. The marked spatial variation in degree of orientation revealed within the two HDPE films A and B studied here, extruded under different cooling conditions, points to the potential of the method in this context.

We are indebted to Van Leer Research Laboratories for financial support and for providing the polyethylene films. We are also grateful to Mr. W. Organ and Dr. G. Reynolds of Van Leer and Dr. I. H. Hall and Professor R. H. Peters of UMIST for helpful discussions. R. J. T. was supported by a Science and Engineering Research Council CASE Research Studentship.

APPENDIX

Analysis for a General Point on the Diffraction Ring. Equations (4) and (5) apply to any point on the diffraction ring. The angle β, however, will vary with position around the ring. Consider unit vectors $\mathbf{S}_0$ and $\mathbf{S}$ parallel to incident and diffracted beams respectively, as indicated in Figure 4. By inspection, $\mathbf{S}$ is given in terms of $\mathbf{S}_0$, $\mathbf{e}_3$ and their mutually perpendicular unit vector $\mathbf{S}_0 \times \mathbf{e}_3$ as follows:

$$\mathbf{S} = \cos 2\theta^1\, \mathbf{S}_0 + \sin 2\theta^1 \cos\phi\, \mathbf{e}_3 + \sin 2\theta^1 \sin\phi\, \mathbf{S}_0 \times \mathbf{e}_3 \tag{13}$$

This can be rewritten in terms of unit vectors $\mathbf{e}_3$ and $\mathbf{e}_2$ and $\mathbf{e}_1$ (parallel and perpendicular to the specimen surface, respectively) by noting that

$$\mathbf{S}_0 = -\sin\alpha^1\, \mathbf{e}_1 + \cos\alpha^1\, \mathbf{e}_2 \tag{14}$$

and substituting into eq. (13)

$$\begin{aligned}\mathbf{S} = {} & (\sin 2\theta^1 \cos\alpha^1 \sin\phi - \cos 2\theta^1 \sin\alpha^1)\mathbf{e}_1 \\ & + (\cos 2\theta^1 \cos\alpha^1 + \sin 2\theta^1 \sin\alpha^1 \sin\phi)\mathbf{e}_2 \\ & + \sin 2\theta^1 \cos\phi\, \mathbf{e}_3\end{aligned} \tag{15}$$

The glancing angle of the diffracted beam β^1 for a general point on the diffraction ring is then given by

$$\sin\beta^1 = \mathbf{S} \cdot \mathbf{e}_1 = \sin 2\theta^1 \cos\alpha^1 \sin\phi - \cos 2\theta^1 \sin\alpha^1 \tag{16}$$

To find the direction of plane normals contributing to a given point on the ring, it is convenient to use the scattering vector $\mathbf{s}$, defined as usual for X-rays of wavelength λ, as follows:

$$\lambda\mathbf{s} = \mathbf{S} - \mathbf{S}_0 \tag{17}$$

Here, however, we note that eq. (16) neglects the small deflections of $\mathbf{S}$ and $\mathbf{S}_0$ due to refraction. For consistency the following argument also neglects these deflections. Substituting from eqs. (14) and

(13) into eq. (17), and noting that one of the geometrical conditions for diffraction is that a diffracting plane unit normal **n** must be parallel to **s**, we find

$$\mathbf{n} = \mathbf{s}/|\mathbf{s}| = (\cos\theta \sin\phi \cos\alpha + \sin\theta \sin\alpha)\mathbf{e}_1 + (\cos\theta \sin\phi \sin\alpha - \sin\theta \cos\alpha)\mathbf{e}_2 + \cos\theta \cos\phi\, \mathbf{e}_3 \quad (18)$$

Crossply-Laminated Film at Edge-On Incidence. Consider the experiment depicted schematically in Figure 4 carried out on a crossply-laminated film, in which c-axis orientation in each layer lies in the $\mathbf{e}_2$, $\mathbf{e}_3$ plane, tilted away from $\mathbf{e}_3$ by an angle $\pm\,\omega$. ($hk0$) plane normals will therefore be confined to planes containing $\mathbf{e}_1$, tilted away from the equatorial plane by an angle $\pm\,\omega$. The locus of ($hk0$) plane normals **n** can therefore be written

$$\mathbf{n} \cdot \mathbf{e}_3 / \mathbf{n} \cdot \mathbf{e}_2 = \pm \tan\omega \quad (19)$$

Combining the two restrictions on **n** given by eqs. (18) and (19), we find the following expression for the azimuthal angle ϕ^* at which ($hk0$) diffraction will appear on the WAXD pattern (taking the limiting case of edge-on incidence $\alpha \rightarrow 0$)

$$\cos\phi^* = \pm \tan\theta \tan\omega \quad (20)$$

References

1. G. W. Schael, *J. Appl. Polym. Sci.*, **8**, 2717 (1964).
2. H. Tanaka, T. Masuko, and S. Okajima, *J. Polym. Sci., A-1*, **7**, 3351 (1969).
3. H. Tanaka, T. Masuko, and S. Okajima, *J. Appl. Polym. Sci.*, **16**, 441 (1972).
4. P. A. Flournoy, *Spectrochim. Acta*, **22**, 15 (1966).
5. C. S. P. Sung, *Macromolecules*, **14**, 591 (1981).
6. N. J. Harrick, *Internal Reflection Spectroscopy*, Interscience, New York, 1967.
7. M. R. Kantz, H. D. Newman and F. H. Stigale, *J. Appl. Polym. Sci.*, **16**, 1249 (1972).
8. Z. Mencik and D. R. Fitchmun, *J. Polym. Sci., Polym. Phys. Ed.*, **11**, 973 (1973).
9. J. Bowman, N. Harris, and M. Bevis, *J. Mater. Sci.*, **10**, 63 (1975).
10. K. Katayama, T. Amano, and K. Nakamura, *Kolloid Z. Polym.*, **226**, 125 (1968).
11. A. Thetford and S. C. Simmens, *J. Microsc.*, **49**, 143 (1969).
12. H. K. Herglotz, "*Characterization of Materials in Research*, Syracuse University Press, Syracuse, 1975, Chap. 5.
13. H. K. Herglotz, *J. Coll. Int. Sci.*, **75**, 105 (1980).
14. A. H. Compton and S. K. Allison, *X-Rays in Theory and Experiment*, Van Nostrand, New York, 1935.
15. A. Keller and M. J. Machin, *J. Macromol. Sci. (Phys.)*, **B1**, 41 (1967).
16. J. A. Ibers and W. C. Hamilton, Eds., *International Tables for X-Ray Crystallography*, Kynoch Press, Birmingham, 1974, Vol. 4.
17. C. W. Bunn, *Trans. Faraday Soc.*, **35**, 482 (1939).

Received August 8, 1983
Accepted February 1, 1984